Determination of temperature and transverse flow velocity at chemical freeze-out in relativistic nuclear interactions

A. D. Panagiotou,* G. Mavromanolakis, and J. Tzoulis
Physics Department, Nuclear and Particle Physics Division, University of Athens, Panepistimiopolis, GR-157 71 Athens, Hellas
(Received 18 July 1995)

We propose a parameter-free method to determine the temperature of a thermalized state in relativistic nuclear interactions, using the experimental μ_q/T and μ_s/T values, obtained from strange particle ratios. The hadron gas formalism and strangeness neutrality are employed to relate the quark-chemical potential μ_q and μ_s to the temperature and thus determine its value at chemical freeze-out. This temperature, together with the inverse slope parameter from m_T distributions, enable the determination of the transverse flow velocity of the fireball matter, thus disentangling the thermal and flow effects. We study several nucleus-nucleus interactions from AGS and SPS and obtain the temperature, transverse flow velocity, and quark-chemical potentials. Extrapolating the systematics we predict the values of these quantities for ongoing and future experiments at AGS, SPS, and RHIC. We discuss the possibility of reaching the conditions for quark deconfinement and QGP formation and give distinct and identifiable signature.

PACS number(s): 25.75.−q, 05.30.Ch, 12.38.Mh, 24.85.+p

I. INTRODUCTION

In the study of relativistic nucleus-nucleus interactions, the determination of the temperature of the produced nuclear state (fireball) is one of the most important tasks. The temperature is a fundamental thermodynamic quantity, entering in the equation of state (EoS) and in the calculation of many other thermodynamic variables, such as the quark-chemical potentials, energy density, entropy, etc.

The estimation of the temperature of compressed and excited nuclear matter is strongly interlaced with its transverse flow. One customarily uses the inverse slope parameter of the fit to the m_T distributions as the "apparent temperature." These distributions, however, suffer from possible flow effects of the compressed nuclear matter, whereby the transverse velocity of the flow motion is added to the thermal velocity, resulting in a larger apparent temperature. This has as a consequence the false increase of all other thermodynamic quantities depended on the temperature, hence the erroneous evaluation of the state reached in a nuclear interaction.

The disentanglement of the thermal and flow effects in m_T distributions was very difficult, since it was based on the use of hydrodynamics models in which many assumptions and the unknown EoS serve as the basic inputs [1]. The m_T spectra give only a correlation between the collective transverse velocity of the fluid and the local temperature, which is difficult to exploit. Therefore, one is unable to prove the existence and give the magnitude of transverse flow from the m_T distributions alone. Only an indirect proof could be given, based on the phenomenological analysis and the hydrodynamics calculations. For example, the concave shape of pion m_T distributions can be reproduced by assuming transverse flow of the fireball matter [2]; it can also be reproduced by allowing higher mass resonances to decay before freeze out.

In this paper we propose [3] a simple a parameter-free method to determine the temperature of the state at chemical freeze-out, that is at the stage where strange particles decouple from nonstrange hadrons and the population of each species remains henceforth unchanged. To achieve this we employ the hadron gas (HG) formalism to interrelate the quantities T, μ_q, μ_s and use the experimental μ_q/T and μ_s/T values, obtained from strange particle ratios, where μ_q and μ_s are the light and strange quark-chemical potentials, respectively.

Comparing the temperature T to the inverse slope parameter, obtained from the corresponding m_T distributions, we can extract the transverse flow velocity, $\beta = v/c$, of the nuclear fluid and disentangle the effects of thermal and collective motion. Note that in our procedure we do not perform any fit to experimental distributions, as one is forced in thermal and hydrodynamics models.

In Sec. II we employ the HG formalism to arrive at the relation between μ_q, μ_s, and T, and describe how this is used to determine the temperature. We also discuss the proposed regions in the phase diagram. In Sec. III we analyze several nucleus-nucleus interactions from AGS at Brookhaven and SPS at CERN and determine the temperature and the transverse flow velocity for each interaction at chemical freeze-out. We also study the systematics of the quantities T, μ_q, and β for these systems and extrapolate the corresponding fits to higher energy, predicting the range of their values for several interactions at RHIC. We discuss the disappearance of transverse flow at low and high incident energies, as well as the onset and complete transparency of nuclear matter. We calculate the energy density for all interactions discussed, employing both the QGP and HG formalisms and compare it to experimental and theoretical values. Finally, we examine the effect of incomplete strangeness saturation on the determination of the temperature and find it to be minimal.

In Sec. IV we discuss our findings in terms of previous suggestions for a possible attainment of the QGP phase in

*Electronic address: apanagio@atlas.uoa.ariadne-t.gr

S-induced interactions at the SPS. On the basis of the systematics of the analyzed data and the empirical extrapolations, we recommend appropriate interactions for studying the phase transition(s) at SPS and RHIC.

Our conclusions are that all interactions at SPS ($S+A$ at 200A GeV) have reached, as an ''average'' event, a temperature $\langle T\rangle\sim 194$ MeV and quark-chemical potentials $\langle\mu_q\rangle\sim 80$ MeV and $\langle\mu_s\rangle\sim 4$ MeV at chemical freeze-out. The close to zero strange quark-chemical potential is consistent with these interactions being very near the region of the HG phase where $\mu_s=0$. Therefore, invoking the formation of QGP for understanding $\langle\mu_s\rangle\sim 0$ in these data is erroneous. Our prediction for the range of T and μ_q in Pb+Pb at SPS (160A GeV) locates this interaction further inside the region of deconfined quark matter. The Au+Au interaction at the AGS (11A GeV), producing about the highest possible nuclear matter density and transverse flow velocity, remains in the HG phase, while at RHIC, it should reach well inside the ideal QGP region. At RHIC, one may also find a baryon-free central region for light ion interactions, such as Ni+Ni at $\sqrt{s}=200A$ GeV.

The systematics of the transverse flow velocity as function of the total c.m. energy ($\sqrt{s}$) for the Au+Au system indicate the disappearance of flow in nuclear matter at both low ($\sqrt{s}\sim 1.4A$ GeV) and very high ($\sqrt{s}\sim 200A$ GeV) energies. Finally, we suggest possible evidence for the existence of a distinctly separate region of deconfined quark matter with correlated, massive and interacting quarks, in between the HG and ideal QGP phases (not a HG-QGP mixed phase). We propose that selected Pb+Pb interactions at 160A GeV may reach this region and produce a state identified by *negative* strange quark-chemical potential.

II. THEORETICAL CONSIDERATIONS

A. The formalism

We begin by considering the grand canonical partition function of the strange particles in the hadron gas formalism (Boltzmann approximation), assuming local thermal equilibration:

$$\ln Z_{\text{strange}}(V,T,\lambda)=\sum_k Z_k\prod_i \lambda_i^k, \tag{1}$$

where the fugacity λ_i^k controls the quark content of the k particle and $i=s,b$ for the strangeness and baryon number ($\lambda_b=\lambda_q^3$), respectively. We neglect in Eq. (1) the isospin asymmetry, assuming $\mu_u=\mu_d=\mu_q$. At first, we also assume full chemical equilibration, setting the chemical saturation factor for strange quarks $\gamma_s=1$. The case of incomplete chemical equilibration will be discussed in Sec. III E.

The one-particle Boltzmann partition function is

$$Z_k(V,T)=(VT^3/2\pi^2)\sum_j g_j(m_j/T)^2K_2(m_j/T)$$
$$=(VT^3/2\pi^2)W(x_k), \tag{2}$$

where $x_j=m_j/T$ and the summation runs over the resonances of each particle species with mass m_j; g_j, the degeneracy factor, counts the spin and isospin degrees of freedom of the j resonance; V is the volume of the system and K_2 is the modified Bessel function. For the mass range of the resonances we have taken all available data: kaons up to 2045 MeV/c^2, hyperons up to 2350 MeV/c^2, and cascades up to 2025 MeV/c^2. The Ω^- resonances are not included since there is only one well-known state at 1672 MeV [4].

Invoking strangeness conservation in strong interactions we have

$$\langle N_s-N_{\bar{s}}\rangle=(\lambda_s/V)\partial/\partial\lambda_s[\ln Z_{\text{strange}}(V,T,\lambda_s,\lambda_q)]=0, \tag{3}$$

$$Z_K(\lambda_s\lambda_q^{-1}-\lambda_s^{-1}\lambda_q)$$
$$+Z_\Xi(\lambda_s\lambda_q^2-\lambda_s^{-1}\lambda_q^{-2})+2Z_\Xi(\lambda_s^2\lambda_q-\lambda_s^{-2}\lambda_q^{-1})=0. \tag{4}$$

Defining the quantity

$$\gamma=\lambda_s/\lambda_q=\exp(\mu_s/T)\exp(-\mu_q/T), \tag{5a}$$

Eq. (4) becomes

$$(2Z_\Xi\lambda_q^6)\gamma^4+[\lambda_q^3(Z_K+Z_Y\lambda_q^3)]\gamma^3$$
$$-(Z_Y+Z_K\lambda_q^3)\gamma-2Z_\Xi=0. \tag{5b}$$

Equation (5) defines the strange quark-chemical potential in terms of μ_q and T:

$$\mu_s/T=\mu_q/T+\ln\gamma. \tag{6}$$

Equation (6) correlates the quark-chemical potentials and the temperature. For example, it gives the allowed values of μ_s/T as function of T, for a certain value of μ_q/T, or, for a specific value of μ_q/T and μ_s/T, it gives a well-defined allowed temperature. We capitalize on this correlation to determine the temperature at chemical freeze-out, T_{ch}, having obtained the values for μ_s/T and μ_q/T from experimental strange particle ratios.

In the HG phase the quark-chemical potentials μ_q and μ_s are coupled through the production of u, d, and s quarks in strange hadrons. Due to this coupling, strangeness conservation does not necessitate $\mu_s=0$ everywhere in the HG phase.[1] It may obtain nonzero values in certain regions. The condition $\mu_s=0$ in Eq. (4) requires $\lambda_s=\lambda_s^{-1}=1$, and it becomes [5]

$$[Z_Y(\lambda_q+\lambda_q^{-1})-Z_k+2Z_\Xi](\lambda_q-\lambda_q^{-1})=0. \tag{7}$$

Note that this equation is independent of Z_Ω, which drops out from Eq. (3). The second factor gives $\mu_s=0$ at $\mu_q=0$ for all T. The first factor gives the range of values of μ_q as function of T, for which $\mu_s=0$ in the baryon-rich HG phase,

$$\mu_q=T\cosh^{-1}(Z_K/2Z_Y-Z_\Xi/Z_Y). \tag{8}$$

This is shown by the solid curve on the $(T-\mu_q)$ plane (phase diagram) of Fig. 1, starting at $T(\mu_q=0)\sim 200$ MeV and ending at $\mu_q(T=0)\sim 600$ MeV.

[1] In a baryon-free state ($\mu_q=0$), $\mu_s=0$ for all T, since there could be no coupling between μ_q and μ_s.

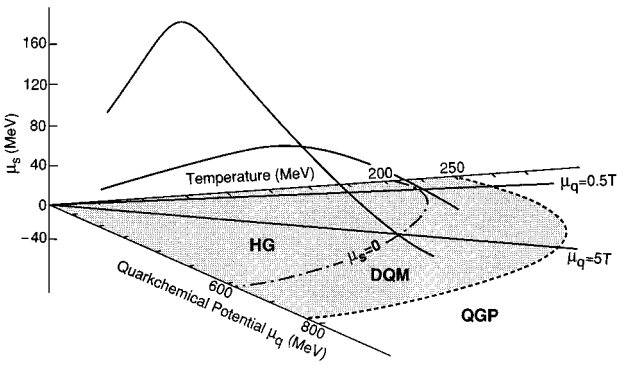

FIG. 1. Variation of μ_s with temperature, Eq. (6), is shown on the vertical plane, formed by the μ_s axis and the lines $\mu_q=0.5T$ and $5T$ on the $(T-\mu_q)$ plane.

B. Definitions of regions in phase diagram

To define the various regions in the phase diagram we consider the two order parameters of statistical QCD [6].

(a) The average thermal Wilson loop $\langle L\rangle$, related to the free energy F of an isolated quark: $\langle L\rangle\sim\exp(-F/T)$. In the confinement region there are no free quarks and F is infinite, making $\langle L\rangle=0$. As color screening sets in progressively, it is possible to separate a $q\bar{q}$ pair and thus F becomes finite. In this regime, $\langle L\rangle$ attains suddenly larger values and subsequently saturates with increasing temperature.

(b) The scalar quark density $\langle\psi\bar{\psi}\rangle$, which provides a measure of the effective quark mass and hence of the chiral symmetry restoration. $\langle\psi\bar{\psi}\rangle>0$ in the confinement regime. It decreases abruptly once deconfinement sets in, reaching asymptotically zero in the ideal QGP phase.

In the phase diagram, we consider the $\mu_s=0$ curve as the *upper limit* of the HG phase [5]. Statistical QCD and strong interaction phenomenology suggest a temperature $T_H\sim200$ MeV, at vanishing baryon number density, as a limiting temperature for hadronic physics [6]. Statistical QCD predicts also the onset of deconfinement at a temperature $T_d\sim200$ MeV for $\mu_q=0$. A characteristic of the deconfinement temperature is that it decreases with increasing μ_q in a similar way as the $\mu_s=0$ curve [6]. Lattice QCD calculations, for three-quark flavors at zero baryon density, give a critical temperature for the transition to QGP of order 150 MeV. Experimental evidence, however, suggests that it may not be so low, since the nuclear state formed at this temperature in Si+Au interactions at 14.5A GeV has $\mu_s\sim65$ MeV, much larger than the zero value expected in QGP (see analysis of AGS data in Sec. III A and also Ref. [26]).

We consider the region above the T $(\mu_q=0)\sim O$ (250) MeV phase curve (dashed) as the *lower limit* of the ideal quark-gluon plasma phase. In this region the order parameters $\langle L\rangle$ and $\langle\psi\bar{\psi}\rangle$ are approaching their asymptotic values.

The region between the two curves we define to be the deconfined quark mater (DQM) phase with correlated, massive, and interacting quarks [7]. In transversing this region, the deconfined quarks lose mass, their interaction becoming weaker $(a_s<1)$, achieving the bare quark mass in the ideal QGP phase, where $a_s\sim0$. We thus surmise that, deconfinement and chiral symmetry restoration set in at approximately $T\sim200$ MeV and gradually approach saturation above $T\sim250$ MeV. This picture necessitates the existence of distinctly different domains for the two phases DQM and QGP, as shown in Fig. 1.

What may the $\mu_s=0$ curve signify? In the HG phase and up to this curve, there exists a coupling between the quark-chemical potentials μ_q and μ_s in the produced strange hadrons, giving *positive* values for μ_s. At the crossing of this boundary, this coupling seizes to exist (in *hadrons*) and $\mu_s=0$. This may be taken as sign of deconfinement (vanishing of bag pressure). Beyond, the coupling is still in effect among the *deconfined correlated quarks*, as long as they possess noncurrent masses, but in a different form now, resulting in strongly *negative* strange quark-chemical potential[2] in the DQM phase [8]. In the QGP phase where $q\bar{q}(q=u,d,s)$ are produced independently in pairs, the absence of coupling results in $\mu_s=0$ again throughout this phase. Thus, the $\mu_s=0$ line may be taken as the boundary between the hadronic and deconfined phases. Note that there is no reason forbidding μ_s to obtain negative values, as is the case with μ_q, which can be only positive in nuclear interactions. Negative strange quark-chemical potential has not as yet been observed in interactions (''average'' events) and rightfully so (see Discussion).

In the HG phase, the dependence of the strange quark-chemical potential on μ_q and T, given by Eq. (6), is shown in Fig. 1 on the vertical plane formed by the μ_s axis and chosen lines on the $(T-\mu_q)$ plane, say $\mu_q/T=0.5$ or 5. μ_s starts at zero, attains positive values, and becomes zero again at $T=198$ MeV or 96 MeV, respectively. For higher temperature, μ_s becomes negative in the DQM region. Note that the $\mu_s=0$ curve on the phase diagram, Eq. (8), is the locus of the common points of all μ_s curves, Eq. (6), with the $(T-\mu_q)$ plane.

III. ANALYSIS OF STRANGE PARTICLE DATA

A. Determination of temperature

The variation of μ_s/T with temperature along given (specified by experiment) $\mu_q/T=\alpha\pm\Delta\alpha$ lines, is shown in Fig. 2. We take into account and depict the uncertainty in the experimental value of μ_q/T, in order to study the accuracy in determining the temperature. We note that the uncertainty in the temperature comes exclusively from the uncertainty in the experimental value of μ_s/T, for the cases considered.

Using the prescribed method we analyze several nucleus-nucleus interactions, starting with Si+Au at 14.5A GeV of the E802 experiment at Brookhaven [9]. From the analysis of the K^+, K^-, Λ, $\bar{\Lambda}$ date we find [10]: $\mu_q/T=1.32\pm0.06$, $\mu_s/T=0.46\pm0.08$, $I=196\pm4$ MeV, the inverse slope parameter from the fit to the $K^\pm m_T$ distributions [9].

The dependence of μ_s/T on T along $\mu_q/T=1.32$ is shown in Fig. 2. We observe that, to the experimental value $\mu_s/T=0.46\pm0.08$, corresponds a specific temperature, $T=140\pm5$ MeV. The inverse slope parameter from the m_T

[2]Negative μ_s could be seen as due to the mass spectrum of strange hadrons. The actual shape of the curve in the DQM region is much different if one allows deconfinement and chiral symmetry restoration to set in [8].

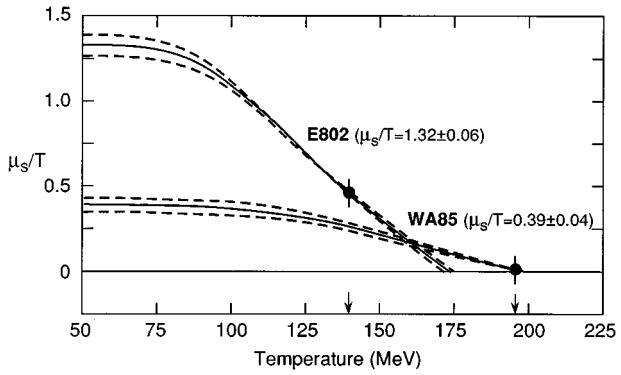

FIG. 2. Dependence of μ_s/T on T for two interactions along the corresponding μ_q/T lines. The experimental μ_s/T values and corresponding temperatures are indicated.

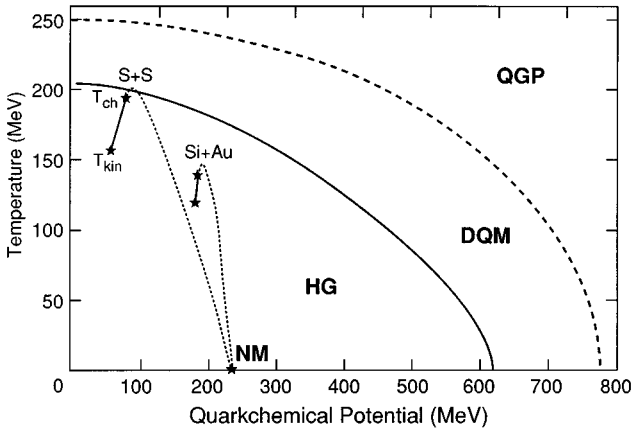

FIG. 3. Phase diagram showing the trajectories followed by the two interactions (see Discussion in the text).

distributions, $I=196$ MeV, is much higher than this temperature, indicating the existence of a large blue shift of about 40%, caused by the transverse flow of the fireball matter. We shall discuss this in the next subsection.

The $S+W$ interaction at 200A GeV, studied at CERN by the WA85 experiment [11] is analyzed next and we find [7]: $\mu_q/T=0.39\pm0.04$, $\mu_s/T=0.033\pm0.07$, $I=234\pm11$ MeV, the inverse slope parameter from the strange baryon m_T distributions [11]. Figure 2 shows the variation of μ_s/T with temperature along the $\mu_q/T=0.39\pm0.04$ line. Observe again that, to the experimental value $\mu_s/T=0.033\pm0.07$, corresponds a specific temperature, $T=196\pm9$ MeV. In this interaction there is a difference between the temperature and the inverse slope parameter of $\sim$38 MeV, caused by substantial transverse flow contribution of about 20% to the thermal effects.

We performed similar analysis of the CERN NA35 [12,10] and NA36 [13,7] strange particle data and determined the temperatures at chemical freeze-out to be in the range $T_{\rm ch}=191$–194 MeV. Table I lists the apparent and flow-corrected thermodynamic quantities for all systems considered.

Intuitively, the maximum temperature, T_0, produced in the fireball of two colliding nuclei should depend on the total energy available in the center-of-mass system, $\sqrt{s}$, divided by the number of participant nucleons sharing this energy:

$$T_0 \propto \sqrt{s}/\text{participant}, \tag{9}$$

where the number of participants is taken to be $A_{pr}[1+1.4(A_{tg}/A_{pr})^{1/3}]$. The temperature we have determined at chemical freeze-out $T_{\rm ch}$ is always lower than T_0. In the phase diagram of Fig. 3 we show the points $(T,\mu_q)_{\rm ch}$ at chemical freeze-out from our calculations and the points $(T,\mu_q)_{\rm kin}$ at kinematic freeze-out for the interactions S+S

TABLE I. Apparent and correct thermodynamic quantities for several interactions obtained from our analysis ($\gamma_s=1$).

Experiment	Apparent Correct	T (MeV) T (MeV)	μ_q (MeV) μ_q (MeV)	μ_s (MeV) μ_s (MeV)	β
E802, Si+Au,	14.5A GeV, $1<y<1.6$				
		196 ± 4	259 ± 13	90 ± 16	
		140 ± 5	185 ± 11	64 ± 11	0.32 ± 0.04
WA85, $S+W$,	200A GeV, $2.3<y<2.8$				
		234 ± 11	92 ± 7	4 ± 8	
		196 ± 9	77 ± 6	3 ± 7	0.18 ± 0.06
NA36, $S+$Pb	200A GeV, $2.0<y<2.5$				
		214 ± 11	126 ± 21	3 ± 23	
		194 ± 21	114 ± 22	3 ± 21	0.10 ± 0.12
NA35, $S+$Ag,	200A GeV, $1.1<y<2.2$				
		229 ± 11	111 ± 10	8 ± 21	
		191 ± 17	93 ± 11	7 ± 18	0.18 ± 0.1
$S+S$	200A GeV, $1.7<y<2.25$				
		202 ± 11	78 ± 10	7 ± 13	
		192 ± 15	74 ± 10	6 ± 13	0.05 ± 0.09
$p+S$,	200 GeV, $1.7<y<2.25$				
		173 ± 10	64 ± 11	23 ± 27	
		168 ± 38	62 ± 17	23 ± 26	0.03 ± 0.1

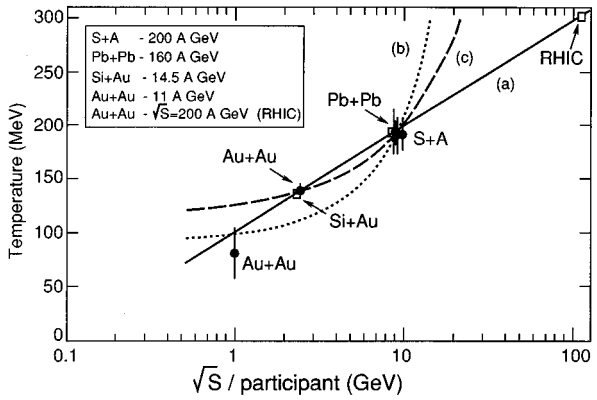

FIG. 4. Temperature vs $[\sqrt{s}/(\text{participant})]$ for several interactions. The small squares indicate predictions for corresponding interactions.

(200A GeV) [2] and Si+Au (14.5A GeV) [14]. The paths drawn for each interaction, starting from cold nuclear matter before collision, are somewhat schematic. We assume that the crossing of phases is accomplished at constant entropy [15]. For S+S at 200A GeV, it is suggestive that the $\mu_s=0$ line, taken to designate the onset of deconfinement, may have been crossed in *some events*, since in the ''average event'' analysis we find $T_{\rm ch}\sim T_d$, the temperature on the $\mu_s=0$ line. This is not the case with Si+Au at 14.5A GeV.

The knowledge of the temperature at chemical freeze-out for interactions at different energies is useful in predicting a lower limit of the maximum temperature T_0 reached in nuclear collisions. This is shown in Fig. 4, where we plot $T_{\rm ch}$ versus $[\sqrt{s}/\text{participant}]$ for the interactions Si+Au at AGS and S+A at SPS. We include also the temperature of the fireball for Au+Au at 1.15A GeV [16], obtained from the study of energy spectra of light particles at midrapidity. The meaning of this plot is the following: in the regions between SPS-AGS and lower, it gives the temperature at chemical freeze-out, while above SPS it predicts the lower limit of T_0 reached in an interaction.

We performed three fits to the data: (a) logarithmic, (b) exponential and (c) linear. An acceptable (least squares) fit and extrapolation is obtained with the logarithmic dependence. On the basis of this empirical fit we predict that the Au+Au interaction at RHIC ($\sqrt{s}=200A$ GeV) and the Pb+Pb interaction at LHC ($\sqrt{s}=5.5A$ Tev) should reach a temperature of at least 300 ± 30 MeV and 450 ± 50 MeV, respectively. For the Pb+Pb interaction at SPS (160A GeV) the predicted temperature at chemical freeze-out, $T_{\rm ch}\sim193$ MeV, is equal to that of the S-induced interactions at 200A GeV. Similar is the case for Au+Au at AGS (11A GeV), for which we predict $T_{\rm ch}\sim139$ MeV, equal to that of Si+Au at 14.5A GeV. These results are summarized in Table II.

For the same colliding nuclei one can study the variation of the (approximate) temperature of the fireball T_0 as function of the total c.m. energy. This is shown in Fig. 5(b) for Au+Au interactions. The lower two points are experimental [16,19], while the others are estimations from Fig. 4 (Table II). Extrapolating, the ''zero temperature'' point is reached at about 6A MeV incident energy, corresponding to the limit for the onset of inelastic scattering for this system.

TABLE II. Thermodynamic quantities obtained from experiments and from our analysis (see text). The (♦) denotes predictions based on the current AGS and SPS data.

Interaction	T (MeV)	μ_q (MeV)	ε(GeV/fm^3) QGP	ε(GeV/fm^3) HG	β
BEVELAC					
Au+Au, 1.15A GeV	81 ± 24	♦ 158 ± 25		♦ 0.26	0.32 ± 0.05
Au+Au, 0.15A GeV	32 ± 10				0.12 ± 0.05
AGS					
Si+Au, 14.5A GeV	140 ± 5	185 ± 11		0.48	0.32 ± 0.04
♦ Au+Au, 11A GeV	139 ± 11	229 ± 40		1.04	0.48 ± 0.23
CERN					
S+Pb, 200A GeV	194 ± 21	114 ± 22	1.9 ± 0.8	2.0	0.1 ± 0.12
S+W, 200A GeV	196 ± 9	77 ± 6	1.9 ± 0.3	1.7	0.18 ± 0.06
S + Ag, 200A GeV	191 ± 17	93 ± 11	1.8 ± 0.5	1.6	0.18 ± 0.1
S+S, 200A GeV	192 ± 15	74 ± 10	1.8 ± 0.5	1.5	0.05 ± 0.09
♦ Pb+Pb, 160A GeV	193 ± 17	161 ± 32	2.0 ± 0.7	3.3	0.33 ± 0.2
♦ Pb+Pb, 80A GeV	178 ± 15	180 ± 34	1.7 ± 0.5	2.4	0.37 ± 0.2
♦ Pb+Pb, 40A GeV	164 ± 12	199 ± 36	1.3 ± 0.5	1.7	0.41 ± 0.2
♦ Ag+Ag, 200A GeV	197 ± 17	120 ± 28	2.0 ± 0.7	2.5	0.23 ± 0.17
♦ Ni+Ni, 200A GeV	197 ± 17	88 ± 25	1.9 ± 0.6	1.9	0.16 ± 0.16
RHIC					
♦ Au+Au, $\sqrt{s}=200A$ GeV	303 ± 30	21 ± 20	14.6 ± 7		$0.0\pm0.1/0$
♦ Ag+Ag, $\sqrt{s}=200A$ GeV	303 ± 30	$0.0\pm19/0$	14.6 ± 7		$0.0\pm0.1/0$
♦ Ni+Ni, $\sqrt{s}=200A$ GeV	303 ± 30	0.0	14.6 ± 7		0.0
♦ Au+Au, $\sqrt{s}=100A$ GeV	270 ± 27	58 ± 23	10 ± 4		$0.1\pm0.15/0.1$
♦ Au+Au, $\sqrt{s}=50A$ GeV	240 ± 23	96 ± 26	7 ± 3		0.2 ± 0.16

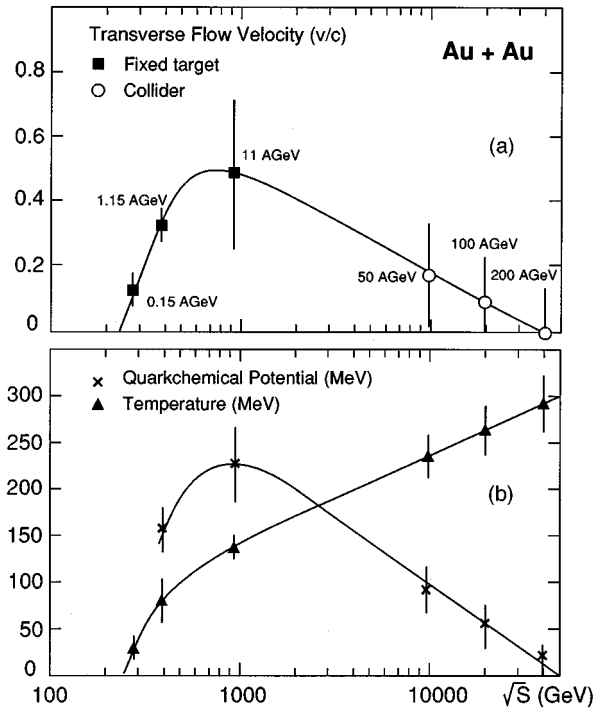

FIG. 5. Transverse flow velocity (a) and quark-chemical potential, temperature (b) vs $\sqrt{s}$ for Au+Au. The lines are to guide the eye.

B. Transverse flow

The compression of nuclear fluid at the initial stage of the nucleus-nucleus collision results in an outward flow of the participant matter. The induced transverse flow velocity contributes a component to the m_T distributions, in addition to the thermal effects. This causes the inverse slope parameter of the fit to the m_T distributions to be larger than the temperature. Thermal and transverse flow effects are very difficult to disentangle, since several thermodynamic variables and the EoS used, are unknown. One can, however, determine the flow velocity, $\beta = v/c$, if one knows the temperature T and the inverse slope parameter I. This is done using the Doppler shift formula, which interrelates the two quantities:

$$T = I\sqrt{[(1-\beta)/(1+\beta)]}$$

$$\beta = [1-(T/I)^2]/[1+(T/I)^2]. \tag{10}$$

For Si+Au at 14.5A GeV ($I = 196$ MeV, $T_{\rm ch} = 140$ MeV) we calculate the transverse flow velocity to be $\beta = 0.32 \pm 0.04$. It is a strong flow, which indicates a high degree of compression of the participant nuclear matter. For $S+W$ at 200A GeV ($I = 234$ MeV, $T_{\rm ch} = 196$ MeV), the transverse flow velocity is found to be $\beta = 0.18 \pm 0.06$, which is about half that of the Si+Au interaction, due to the higher incident energy and consequently higher degree of transparency of nuclear matter.

For Si+Au at 14.5A GeV, hydrodynamics model calculations [2], assuming local thermalization of the collision zone and subsequent hydrodynamic expansion at constant entropy, have hinted, in fitting pion and kaon m_T distributions, the necessity for transverse flow with velocity $\beta = 0.40$–0.45. For the same experiment, calculations using a thermal model, incorporating longitudinal and transverse motion and fitting the rapidity and transverse momentum distributions, estimate the transverse flow velocity at *kinematic freeze-out* to be $\langle\beta\rangle = 0.33$–$0.39$ [14].

Light ion interactions at high energies should exhibit very small collective transverse flow of the participant matter, due to the compression of less nuclear matter and to the higher transparency. This should result in the nearing of the temperature to the inverse slope parameter. We find this to be the case in $S+S$ collisions at 200A GeV [12], for which $T_{\rm ch}$ (192 MeV) $\sim I$(202 MeV) and $\beta = 0.05 \pm 0.09$. To carry this point further we considered the $p+S$ interaction at 200 GeV [12]. We can *a priori* assume that the transverse flow is null, resulting in the equality of the temperature and the inverse slope parameter. Analysis of the strange particle data for this interaction give $\beta \sim 0.03$, having set the strangeness saturation factor $\gamma_s = 1$. Note that, if we require β to be exactly zero, then $\gamma_s \sim 0.4$, a value consistent with a hot hadron gas (see also Discussion in Sec. III E).

For $S+S$ at 200A GeV, hydrodynamic model calculations [1,2] fitting m_T distributions of mesons and baryons, treating β and T as variables, result in a band with many (β, T) pairs instead of a single point. The best estimate is $T \sim 157$ MeV and $\langle\beta\rangle \sim 0.25$–$0.3$, independent of the EoS used, hadron resonance gas or quark-gluon plasma. In a thermal approach [17] for the same interaction, the model parameters T, μ_q, μ_s, and γ_s cannot be determined independently but through a set of nonlinear equations fitting the experimental strange particle ratios. The scenario closest to our analysis [midrapidity $C(2.0)$] gives $T_{\rm ch} = 178$ MeV and $\beta = 0.13$ at chemical freeze-out.

Considering the variation of β in the interactions studied, intuitively we anticipate the compression of nuclear matter (correspondingly the transverse flow) to be inversely proportional to the total energy available per participant nucleon in the center-of-mass system, divided by the number of participants,

$$\beta \propto [\sqrt{s}/(\text{participant})^2]^{-1}. \tag{11}$$

The quantity in the brackets may be thought of as the *transparency parameter* of nuclear matter. In Fig. 6(a) we plot β versus $[\sqrt{s}/(\text{participant})^2]$ for $S+A$ (200A GeV) and Si+Au (14.5A GeV). We fitted the data with three functions: (a) logarithmic, (b) exponential, and (c) linear. Logarithmic and exponential functions give about equally good least squares fit. Based on the logarithmic fit we find for Au+Au (11A GeV) a transverse flow $\beta \sim 0.48$. Note that RQMD calculations for this interaction [18] predict $\beta \sim 0.5$. For Au+Au at RHIC ($\sqrt{s} = 200A$ GeV), the predicted flow is null, $\beta \leqslant 0.003$, indicating an almost transparent nuclear matter. This is more pronounced for lighter nuclei, such as Ag+Ag or Ni+Ni (see also next subsection). For Pb+Pb at 160A GeV we predict a transverse flow velocity $\beta \sim 0.33$, similar to that calculated for Si+Au at 14.5A GeV, Table II.

In nucleus-nucleus collisions we expect the compression of nuclear matter, hence the transverse flow velocity, to increase with increasing incident energy up to the point where nuclear transparency sets in. Then increasing the energy further, both compression and transverse flow should decrease

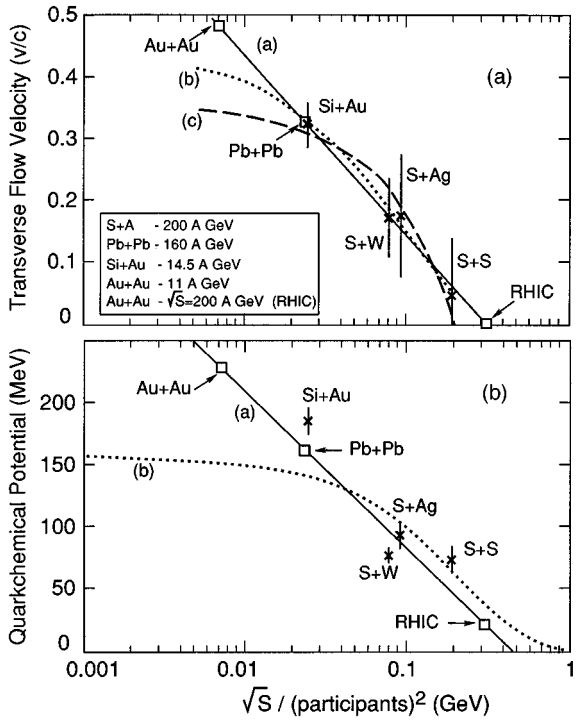

FIG. 6. Transverse flow velocity (a) and quark-chemical potential (b) vs $[\sqrt{s}/(\text{ participant})^2]$ for several interactions. The small squares indicate predictions for corresponding interactions.

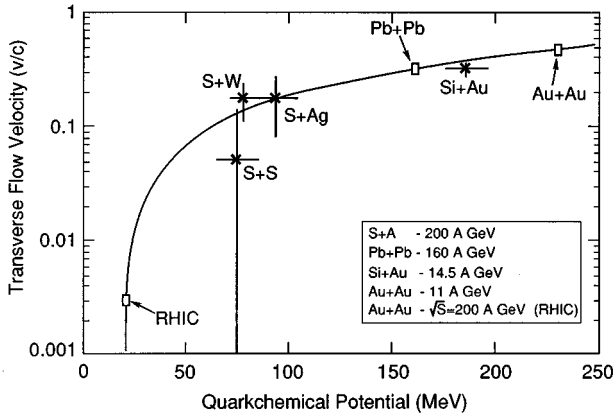

FIG. 7. Transverse flow velocity vs quark-chemical potential for the interactions of Fig. 6.

and became null at the energy where complete nuclear transparency is in effect. It should be noted that this trend is a combined effect of the incident energy and the participant mass of the colliding system. For the same colliding system, an asymmetric bell-shape variation should be seen as function of $\sqrt{s}$ alone. In Fig. 5(a) we show that this is indeed the case for the Au+Au system. We plot the Au+Au (1.15A GeV [16] and 0.15A GeV [19]) data and the predicted values from the previous fit of Fig. 6 at $\sqrt{s}=50$, 100 , and 200A GeV. The trend is clear: as the energy increases the transverse flow of nuclear matter increases; it reaches a maximum in the region $\sqrt{s}\sim 4$–$5A$ GeV and then decreases at higher energies. For Au+Au, it suggests an energy $\sqrt{s}\sim 1.35A$ GeV for the disappearance of transverse flow at low energy, in accordance with other experimental evidence [20]. The disappearance of flow at high energy is suggested to occur at $\sqrt{s}\sim 200A$ GeV. From the systematics it appears that the highest possible transverse flow velocity of nuclear matter is of order $0.5c$.

We should point out here that, due to the particular behavior of the $\mu_s/T=f(T)$ curve throughout the phase diagram, the transverse flow should decrease upon entering the DQM region and become zero in the ideal QGP region [8].

C. Quark-chemical potential

The quark-chemical potential, μ_q, of a nuclear matter fireball represents the baryon number concentration. This in turn depends on the matter density (compression). We anticipate, therefore, the quark-chemical potential to be inversely proportional to the total energy available per participant in the center-of-mass system, divided by the number of participant nucleons, as in the case of the transverse flow velocity,

$$\mu_q \propto [\sqrt{s}/(\text{participant})^2]^{-1}.$$

We have fitted the experimental data with two functions: (a) logarithmic and (b) exponential, Fig. 6(b). We accept the logarithmic dependence as more representative of the data and giving a realistic extrapolation. For the Au+Au interaction at RHIC ($\sqrt{s}=200A$ GeV) we find $\mu_q\sim 21\pm 20$ MeV, which corresponds to an almost transparent nuclear matter (see previous subsection). If lighter ions are chosen, Ag+Ag or Ni+Ni, the quark-chemical potential is predicted to be zero. This is in contradiction to RQMD [21] and dual parton model [22] calculations, which predict high baryon density at midrapidity. If the energy is decreased to $\sqrt{s}=100A$ GeV or 50A GeV, the quark-chemical potential at midrapidity increases to $O(60$ MeV) or $O(100$ MeV), respectively. For the Pb+Pb at 160A GeV we predict $\mu_q\sim O(160$ MeV), increasing to $O(180$ MeV) at 80A GeV and to $O(200$ MeV) at 40A GeV incident energy. The results of our estimations are listed in Table II.

Since both β and μ_q appear to have the same (logarithmic) dependence on the quantity $[\sqrt{s}/(\text{ participant})^2]$ we plot β versus μ_q in Fig. 7. This linear relation between β and μ_q should be considered only in a ''dynamic'' sense in nucleus-nucleus collisions. It has no meaning in ''static'' cases, such as cold nuclear matter. Using this curve we can estimate the quark-chemical potential for certain other interactions for which we know the transverse flow velocity. For Au+Au at 1.15A GeV ($\beta=0.32$) we find $\mu_q\sim 158$ MeV.

In Fig. 5(b) we show the systematics of the quark-chemical potential for Au+Au as a function of $\sqrt{s}$. The maximum value of $\mu_q\sim O(230$ MeV) is achieved at $\sqrt{s}\sim 4$–$5A$ GeV, with corresponding baryon density $\rho\sim 5\rho_0$. Extrapolation of this curve to zero incident energy has no meaning, since we arrive at the ''static'' case.

If our predictions of T and μ_q for Au+Au (11A GeV) and Pb+Pb (160A GeV) interactions are substantiated by the ongoing experiments, the extrapolation to RHIC and LHC energies will be more precise and secure. For the time being we show in Fig. 8 the currently predicted regions on the

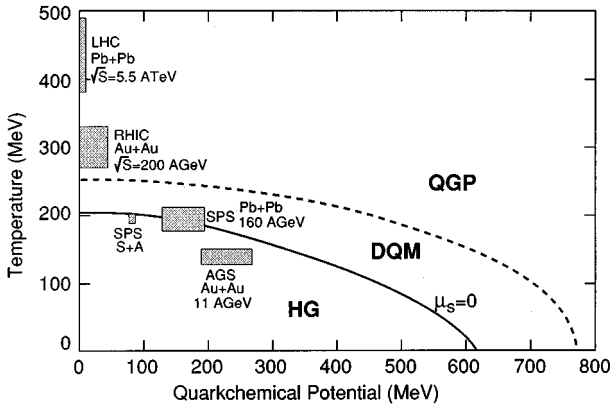

FIG. 8. Phase diagram with the regions predicted to be reached by the ongoing and future interactions at the AGS, SPS, RHIC, and LHC accelerators.

phase diagram reached by several interactions at Brookhaven and CERN.

D. Energy density

In our analysis we have determined the temperature and quark-chemical potentials at chemical freeze-out for several nucleus-nucleus interactions. The values of these quantities may be used to give a lower estimate of the energy density created in each interaction. In the QGP formalism, taking gluons and three-quark flavors, the energy density is

$$\begin{aligned}\varepsilon(\mu_q,T)_{\mathrm{QGP}}=&(37/30-11a_s/3\pi)\pi^2T^4\\&+(1-2a_s/\pi)3\mu_q^2T^2\\&+[3(1-2a_s/\pi)/2\pi^2]\mu_q^4+B\\&+\gamma_s[(18T^4/\pi^2)(m_s/T)^2K_2(m_s/T)\\&+6(m_sT/\pi)^2(m_s/T)K_1(m_s/T)],\end{aligned}\quad(12)$$

where $K_n(m/T)$ is the modified Bessel function of order n and B the MIT bag model vacuum energy density. Taking $a_s\sim0.6$ and $\gamma_s\sim0.4$, 0.6 for Au+Au (11A GeV) and Pb+Pb (160A GeV), respectively, and $a_s\sim0.2$, $\gamma_s\sim1$ for RHIC, we estimate the corresponding values of the energy density listed in Table II. The relative contribution of strange quarks to the energy density in the baryon-free ideal QGP region (RHIC, LHC) amounts to about 35%, almost independent of the temperature in this range.

We have also calculated the energy density of the interactions at AGS and SPS in the HG formalism, deriving the relation from the total partition function, including both strange and nonstrange hadrons:

$$\varepsilon(\mu_q,T)_{\mathrm{HG}}=(T^2/V)\partial/\partial T[\ln Z(V,T,\lambda_s,\lambda_q)],\quad(13)$$

where the nonstrange meson and baryon resonance masses extent to 2340 MeV and 2600 MeV, respectively.

For $S+A$ (200A GeV) the mean value of the energy density is: $\varepsilon_{\mathrm{QGP}}=1.8$ GeV/fm^3 and $\varepsilon_{\mathrm{HG}}=1.7$ GeV/fm^3. Note that, for $a_s\sim0.2$–0.0 appropriate for the ideal QGP, we find $\varepsilon_{\mathrm{QGP}}\sim3.0$–$3.3$ GeV/fm^3. The equality of $\varepsilon_{\mathrm{QGP}}(a_s\sim0.7)$ and $\varepsilon_{\mathrm{HG}}$ may suggest (from another point of view) that we are at present at the phase boundary between HG and DQM and that a distinct region of deconfined quark matter with large a_s values should exist. Thus, an interaction should not go directly from the HG ($a_s>0.7$) to the ideal QGP ($a_s<0.2$) phase, but through a transition region with $1>a_s>0$.

For the $S+A$ interactions at the SPS, the calculated mean energy density is $\langle\varepsilon\rangle\sim1.8$ GeV/fm^3. It agrees with calculations from experimental dN/dy distributions using the Bjorken approach with a (more realistic) formation time, $\tau_0\sim1.5$ fm/c. The Pb+Pb interaction at 160A GeV should reach $\langle\varepsilon\rangle>2$ GeV/fm^3 for selected events with high T and μ_q. It will also produce global thermal equilibrium, a situation where the notion of ''energy density'' is really applicable. If the critical energy density for deconfinement, as given by lattice QCD, is of order 2 GeV/fm^3, then we are very close.

Estimates of the energy density in Au+Au collisions expected at RHIC have been given by Satz [23]. The energy density is calculated assuming free flow (Bjorken approach) and extrapolating to $(dN/dy)_{AA}$ from systematics of pp collisions up to Tevatron energies. Using as rescattering parameter $\alpha=1.1$, the energy density is found to be of $O(5)$ GeV/fm^3, a value about three times smaller than our calculation for an ideal QGP with three-quark flavors. However, as stated in this reference, ε could increase by a factor 3–4 if $\alpha\sim\frac{4}{3}$, as suggested by several event generators and if the isentropic approach [24] is used. This will bring it in accord with our estimation.[3]

E. Partial strangeness equilibration

In our procedure to determine the temperature we have neglected the possibility for partial strangeness equilibration, having set the strangeness saturation factor $\gamma_s=1$ in Eq. (1). To study the effect of $\gamma_s<1$ we consider the WA85 data, which permit the calculation of γ_s in the HG formalism:

$$\gamma_s=[(\Xi^-/\Lambda)(\Xi^+/\overline{\Lambda})]^{1/2}/[W(x_\Xi)/W(x_\Lambda)].\quad(14)$$

We include γ_s in Eq. (1) and calculate μ_s/T for a limited range of temperatures ($\sim$190–200 MeV), near the temperature of 196 MeV at which WA85 measured the particle ratios [11,7]: $\Xi^-/\Lambda=0.25\pm0.02$ and $\Xi^+/\overline{\Lambda}=0.53\pm0.04$. We find a very slight shift of the curve to the right, which increases the temperature by approximately 2%, as shown in Fig. 9. For the E802 experiment we find a temperature increase by less than 2%, if we use $\gamma_s=0.4$ (for a hot hadron gas) instead of $\gamma_s=1$.

The incomplete saturation of strangeness phase space has no pronounced effect on the estimation of the temperature at chemical freeze-out. We are, therefore, safe in using $\gamma_s=1$ in the study of other interactions as well, without significant error (see also previous discussion on the $p+S$ interaction in Sec. III A).

---

[3]In Ref. [23] an estimate of the temperature at RHIC is obtained using an ideal QGP with three-quark flavors and $\varepsilon=5$ GeV/fm^3. A temperature $T\sim230$ MeV is obtained, which is about 75% of our prediction ($\sim$300 MeV) based on the empirical fit to $A+A$ data. An increase of ε by the said factor of about 3 will equate the two temperature predictions.

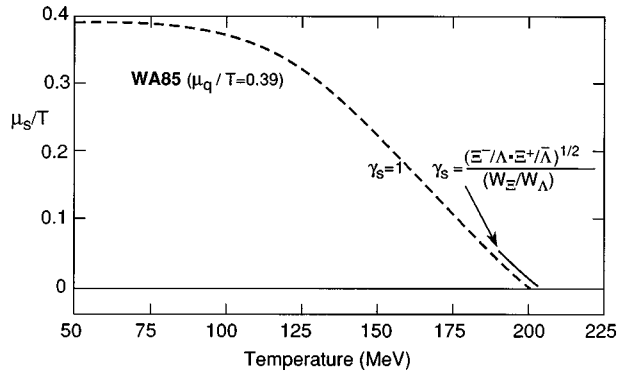

FIG. 9. The effect of using incomplete strangeness saturation, $\gamma_s<1$, on the determination of the temperature for WA85 interaction.

IV. DISCUSSION

A. Strangeness and QGP formation

In the search for quark-gluon plasma via ultrarelativistic nucleus-nucleus collisions, the essential quantities determining whether an interaction has proceeded through a phase transition are the temperature, the quark-chemical potentials μ_q, μ_s, and the strangeness equilibration γ_s, of the state [5,7]. Strange particle ratios can only determine accurately the quantities μ_q/T and μ_s/T. Consequently, an overestimation of the temperature is passed over to the other thermodynamic quantities, leading to erroneous interpretation of the data. Figure 10(a) shows a sector of the phase diagram and the (T,μ_q) points for several interactions. As ''temperature,'' the inverse slope parameter is used. A number of obvious discrepancies are noted, stemming from the incorrect location of the points:

(i) All S-induced interactions at 200A GeV have μ_s very small, $\langle\mu_s\rangle\sim 5.5$ MeV, while their inverse slope parameters are very different, by as much as 40 MeV.

(ii) The Si+Au interaction at 14.5A GeV with $\mu_s=90$ MeV has an apparent location in the same region of the phase diagram as the S-induced interactions at 200A GeV with $\langle\mu_s\rangle\sim 5.5$ MeV.

The transverse flow-corrected (T,μ_q) points from our analysis are shown in Fig. 10(b). The discrepancy between the apparent points is now removed and an order is established: all S-induced interactions at 200A GeV have similar temperature, $\langle T\rangle\sim 194\pm 7$ MeV, and strange quark-chemical potential $\langle\mu_s\rangle\sim 4.5\pm 8$ MeV, in accordance with all points being very near the $\mu_s=0$ curve, on the HG side. The Si+Au interaction at 14.5A GeV is located in the core of the HG region, far from the $\mu_s=0$ curve.

The interpretation of the apparent thermodynamic quantities of the WA85 experiment arouse considerable interest and speculation as to whether they suggest that the QGP state is approached [5,7]. The main reasons were the very small value of μ_s and the apparent location of the (T,μ_q) point far from the $\mu_s=0$ curve in the HG. Our present analysis removes the latter by relocating the (T,μ_q) point at its correct position, *just below* the $\mu_s=0$ curve, hence, justifying the $\mu_s\geqslant 0$ experimental value without invoking the necessity for QGP formation in these interactions (average event). Considering the entropy per baryon observed ($\sim$35) [12], compared

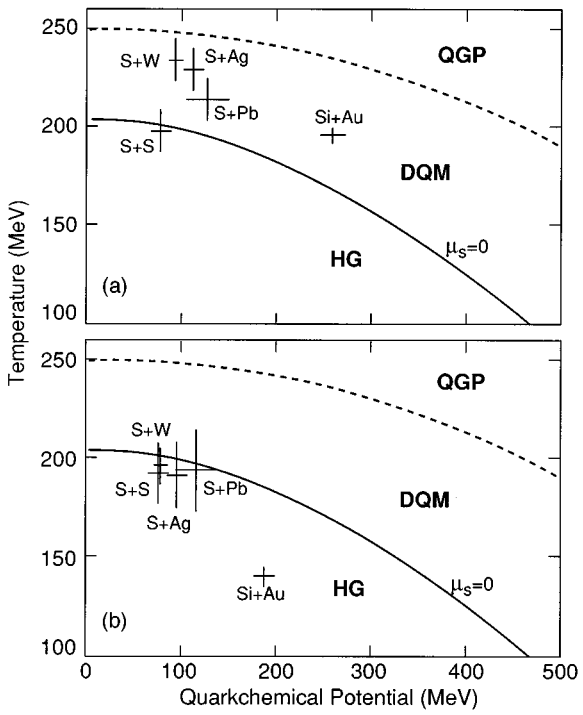

FIG. 10. A sector of the $T-\mu_q$ phase diagram with the apparent $(T-\mu_q)$ values (a) and flow-corrected $(T-\mu_q)$ values (b), for several interactions.

to calculations for HG ($\sim$25) and QGP ($\sim$60) [5] and the substantial strangeness equilibration $\gamma_s=0.58$ [7], it is suggestive that some events have crossed the $\mu_s=0$ line into the deconfinement region. This should be seen more clearly in carefully selected events and the signature would be the observation of $\mu_s<0$.

B. Recommendations for interactions at SPS and RHIC

Examining the predictions of Table II we can make the following recommendations for the more appropriate and interesting interactions at SPS and RHIC.

At SPS, the interaction Pb+Pb at 160A GeV appears to reach simultaneously the highest temperature and quark-chemical potential in the fireball, intruding furthest inside the deconfined quark matter domain. All other interactions at lower energy or with lighter projectile target will be at an equal or less advantaged position. An equally good interaction is Ag+Ag at 200A GeV.

At RHIC, the interaction Ag+Ag and more so Ni+Ni at $\sqrt{s}=200A$ GeV, should produce a baryon-free midrapidity. This will result in a stronger concentration of the baryon number in the fragmentation rapidity, thereby exotic ''Centauro'' events and strangelets may be formed [25]. If the energy is reduced to $\sqrt{s}\sim 50A$ GeV, the Au+Au interaction should produce a state with high temperature ($T\sim 240$ MeV) and substantial quark-chemical potential ($\mu_q\sim 100$ MeV). This energy will then facilitate the study of baryon-rich QGP in the central region. Thus RHIC will enable the study of the decrease and disappearance of nuclear opacity at the high energy end.

At RHIC in an environment with $\mu_q\sim 0$, it appears that all nucleus-nucleus interactions at the same incident energy pro-

duce the same temperature and energy density. Therefore, if one wishes to change the energy density, the only way is to change the colliding energy, contrary to the suggestions in [23]

V. SUMMARY AND CONCLUSIONS

In summary, we have determined the temperature at chemical freeze-out using a parameter-free method and the experimental $\mu_q/T, \mu_s/T$ values obtained from strange particle ratios. We have also established the existence and determined the magnitude of the transverse flow for several $A+A$ interactions at AGS and SPS, thus disentangling the (so far elusive) flow from the thermal effects. We have plotted the determined temperatures and transverse flow velocities, quark-chemical potentials as function of the empirical quantities $[\sqrt{s}/(\text{participant})]$ and $[\sqrt{s}/(\text{participant})^2]$, respectively, and have predicted the corresponding values for the ongoing and future experiments at AGS, SPS, and RHIC.

Based on our analysis, empirical fits, extrapolations, and evaluation we put forth the following:

At SPS, the S-induced collisions at 200A GeV indicate that we have reached (in an average event) the upper limit of hadronic physics. Some selected events should have passed the threshold of the quark deconfinement region. At AGS, the Si+Au interaction is far from it.

The Au+Au at 11A GeV is still far from the deconfined state, whereas Pb+Pb at 160A GeV will be in the ''doorway'' of the deconfined phase. An indisputable indication of this would be the observation of large negative strange quark-chemical potential in selected events.

At RHIC, the Au+Au interaction at $\sqrt{s}=200A$ GeV is well inside the ideal QGP phase, with an almost vanishing baryochemical potential.

Ni+Ni interactions at $\sqrt{s}=200A$ GeV should present a baryon-free midrapidity, concentrating the baryon number in the fragmentation region and presenting the possibility for ''Centauro'' events and strangelets. On the other hand, Au+Au at $\sqrt{s}\sim 50A$ GeV will produce a baryon-rich central region. Thus, nuclear interactions at RHIC will enable the study of the variation of transparency of nuclear matter with incident energy.

Equally important, the determination of the collective variables temperature, energy density and transverse flow velocity, will help achieve a reliable hydrodynamic description of nuclear collisions, essential in determining the yet unknown EoS of nuclear matter.

ACKNOWLEDGMENTS

We wish to thank G. Vassiliadis for a critical reading of the manuscript and M. Gazdzicki for interesting and enlightening discussions.

[1] E. Schnedermann, J. Sollfrank, and U. Heinz, Phys. Rev. C **48**, 2462 (1993).

[2] E. Schnedermann and U. Heinz, Phys. Rev. C **50**, 1675 (1994); K. S. Lee, U. Heinz, and E. Schnedermann, Z. Phys. C **48**, 525 (1990).

[3] A. D. Panagiotou, G. Mavromanolakis, and J. Tzoulis, in *Strangeness in Hadronic Matter*, edited by J. Rafelski, AIP Conf. Proc. No. 340 (AIP, New York, 1995), p. 449.

[4] Particle Data Group, Phys. Rev. D **45**, 1 (1994).

[5] M. N. Asprouli and A. D. Panagiotou, Phys. Rev. D **51**, 1086 (1995).

[6] H. Satz, Proc. XXIII Int. Con. High Energy Physics, 1986, Berkeley; L. D. McLerran, and B. Svetitsky, Phys. Lett. **98B**, 195 (1981); J. Kuti, J. Polonyi, and K. Szlachanyi, *ibid.* **98B**, 199 (1981).

[7] M. N. Asprouli and A. D. Panagiotou, Phys. Rev. C **51**, 1444 (1995).

[8] A. D. Panagiotou, G. Mavromanolakis, and J. Tzoulis, Report No. UA/NPPD-21-95 (submitted to Phys. Rev. Lett.)

[9] E802 Collaboration, Y. Akiba *et al.*, Nucl. Phys. **A566**, 269c (1994); **A566**, 457c (1994).

[10] To obtain μ_q/T and μ_s/T the strange particle ratios $(K^+/K^-)^{1/6}(\Lambda/\bar{\Lambda})^{-1/6}$ and $(K^+/K^-)^{-1/3}(\Lambda/\bar{\Lambda})^{-1/6}$ are used, respectively.

[11] WA85 Collaboration, S. Abatzis *et al.*, Nucl. Phys. **A566**, 225c (1994).

[12] NA35 Collaboration, J. Baechler *et al.*, Z. Phys. C **58**, 367 (1993); NA35 Collaboration, T. Alber *et al.*, *ibid.* **64**, 195 (1994).

[13] NA36 Collaboration, E. Andersen *et al.*, Nucl. Phys. **A566**, 217c (1994); NA36 Collaboration, E. Andersen *et al.*, Phys. Lett. B **327**, 433 (1994).

[14] P. Braun-Munzinger, J. Stachel, J. P. Wessels, and N. Xu, Phys. Lett. B **344**, 43 (1995).

[15] A. Leonidov *et al.*, Phys. Rev. D **50**, 4657 (1994).

[16] EOS Collaboration, M. A. Lisa *et al.* (unpublished).

[17] J. Sollfrank, M. Gazdzicki, U. Heinz, and J. Rafelski, Z. Phys. C **61**, 659 (1994).

[18] M. Hofmann *et al.*, Nucl. Phys. **A566**, 15c (1994).

[19] FOPI Collaboration, C. Kuhn *et al.* (unpublished).

[20] D. Krofcheck *et al.*, Phys. Rev. C **46**, 1416 (1992); W. M. Zhang *et al.*, *ibid.* **42**, R491 (1990).

[21] H. Sorge, H. Stocker, and W. Greiner, Ann. Phys. (N.Y.) **192**, 266 (1989); Th. Schonfeld *et al.*, Nucl. Phys. **A544**, 439c (1992).

[22] A. Capella, C. Merino, and J. Tran Thanh Van, Nucl. Phys. **A544**, 581cc (1992).

[23] H. Satz, Nucl. Phys. **A544**, 371c (1992).

[24] R. C. Hwa and K. Kajantie, Phys. Rev. D **32**, 1109 (1985).

[25] A. D. Panagiotou, A. Petridis, and M. Vassiliou, Phys. Rev. D **45**, 3134 (1992); M. N. Asprouli, A. D. Panagiotou, and E. Gladysz-Dziadus, Astropart. Phys. **2**, 167 (1994); E. Gladysz-Dziadus and A. D. Panagiotou, in *Strangeness and Quark Matter*, Proceedings of the International Symposium, Krete, September 1994, edited by G. Vassiliadis, A. D. Panagiotou, B. S. Kumar, and J. Madsen (World Scientific, Singapore, 1995), p. 265.

[26] N. Bilic, J. Cleymans, and M. D. Scadron, Int. Jour. Mod. Phys. A **10**, 1169 (1995).